KSCE Journal of Civil Engineering (2018) 22(4):1496-1505
DOI 10.1007/s12205-017-2002-y

Hydraulic Engineering
pISSN 1226-7988, eISSN 1976-3808
www.springer.com/12205

Effect of Debris on Piers Group Scour: An Experimental Study

Ebrahim Rahimi*, Kourosh Qaderi, Majid Rahimpour***, and Mohammad Mehdi Ahmadi******

Received December 17, 2016/Accepted April 18, 2017/Published Online June 14, 2017

Abstract

Debris accumulation upstream of bridge piers is a destructive agent against the piers stability. In this study, the effect of debris geometrical characteristics on the local scour at piers group was investigated. A large set of experimental tests were conducted to investigate the effect of piers configurations, as well as, the shape, thickness, length, and position of debris on the dimensions of scour hole. The results showed that the debris with rectangular shape caused the most scour depth. In addition, among the different configurations of bridge piers, the group piers (2 × 2) demonstrated the largest scour hole. In this configuration, high complex interactions occurred among the flow, sediment and piers which generated strong horseshoe and wake vortices around the piers. The observations showed that the maximum depth of scour hole increases as the debris thickness increases. In addition, more the debris effective length, more the depth of scour hole. In the case of debris with rectangular shape, as the relative thickness of debris increased from 0.5 to 2.67, the depth of scour hole increased 67%, 80%, 84% and 104%, in single, side by side, tandem, and group piers (2 × 2), respectively. By increasing the distance of debris from the water surface, the depth of scour hole increased at the first, and then decreased when the relative submergence depth of debris became 0.46. In this condition, the debris acted as a collar, prevented the bed from scour. The measured scour depths were compared with common empirical formula, the formula were modified by considering the experimental results of this study.

Keywords: *piers group, local scour, debris, geometrical characteristics, experimental study*

1. Introduction

Bridges are among the most important hydraulic structures that are exposed to several destructive agents such as pier scour and hydrodynamic loadings induced by floods or debris accumulation in front of bridge piers. Floating debris caught by bridge piers may cause a large obstruction to flow, accelerate the scour processes and even lead to the bridge failure. In the case of piers group, the probability of debris trapping in front of bridge piers increases significantly, resulting in flooding, damaging loads or excessive scour at bridge foundations. The size and shape of debris accumulation may change from a small cluster of debris upstream of bridge pier to a near complete obstruction of a bridge waterway opening (Lagasse *et al.,* 2010). Debris accumulation geometry depends on the flow condition, channel geometry, pier shape and characteristics of transported debris (Melville and Coleman, 2000).

Although, the effect of debris on the scour process around a single pier has been studied by several researchers (Laursen and Toch, 1956; Melville and Dongol, 1992; Braudrick *et al.*, 1997; Diehl, 1997; Wallerstein, 2003; Lyn *et al.,* 2003; Bradley *et al*., 2005; Zevenbergen *et al.*, 2006; and Briaud *et al.*, 2006), to the author's knowledge, there is no research that has investigated the effects of debris on piers group scour.

Laursen and Toch (1956) investigated the effect of debris accumulation on pier scour and claimed that the scour holes are both deeper and larger in extent than those formed around the pier alone. Based on the data from field surveys, Chang and Shen (1979) performed a statistical analysis of debris hazards to bridges. Melville and Dongol (1992) conducted a series of experiments using a cylindrical debris extending downstream of the bridge pier. They investigated the accumulation effect on equilibrium scour and developed an experimental relationship in which an equivalent bridge pier diameter was defined. Abbe and Montgomery (1996) reported that debris accumulation can cause both constriction and local scour. Diehl (1997) documented that one of the main causes of bridge failures in the USA is due to the debris accumulation. Kattell and Eriksson (1998) reported that debris accumulation is a challenging problem for bridge scour. Mueller and Parola (1998) measured the field pier scour in the presence of debris accumulation. Parola *et al.* (2000) considered the hydrodynamic forces due to debris accumulation. They found that the hydrodynamic forces depend on the blockage ratio and the debris porosity. Richardson and Davis (2001) evaluated the bridge pier scour depth in the case of debris accumulation. Bradley *et al.* (2005) studied the effects of debris impact on

*Ph.D. Candidate, Dept. of Water Engineering, Shahid Bahonar University of Kerman, Kerman, Iran (Corresponding Author, E-mail: rahimi.uk@gmail.com)
**Associate Professor, Dept. of Water Engineering, Shahid Bahonar University of Kerman, Kerman, Iran (E-mail: Kouroshqaderi@uk.ac.ir)
***Associate Professor, Dept. of Water Engineering, Shahid Bahonar University of Kerman, Kerman, Iran (E-mail: Rahimpour@uk.ac.ir)
****Assistant Professor, Dept. of Water Engineering, Shahid Bahonar, University of Kerman, Kerman, Iran (E-mail: ahmadi_mm@uk.ac.ir)

hydraulic structures. Lagasse *et al.* (2010) investigated the impacts of debris on bridge pier scour. Pagliara and Carnacina (2010) performed an experimental study to investigate the effect of debris accumulation at bridge piers and the related scour evolution. Debris with different diameters, roughness and porosity were analyzed. The results showed that the scour depth in the presence of debris accumulation can raise up to three times that without debris accumulation. They found that the effect of debris porosity and roughness on the scour hole geometry is negligible. Based on their investigations, the flow intensity and blockage ratio are the main parameters affecting the temporal scour evolution. Pagliara and Carnacina (2011) studied the effect of frontal shape of woody debris accumulation on scour around bridge piers under the clear water condition. Franzetti *et al.* (2011) designed and built a protection structure consisting of six narrow piles for a bridge pier on the River Po, Italy, to reduce the accumulation of debris material upstream of the piers. The countermeasure devised was a plate that, at the end of flood and moderate flow events, prevented the descent of the debris material accumulated during the peak phase. In this way, the effect of the debris on local scour was avoided in the most dangerous situations for structure stability. Park *et al*. (2016a) studied the effects of debris accumulation at sacrificial piles on bridge pier scour. They proposed new relationships for predicting the bridge pier maximum scour depth in the presence of debris accumulation at sacrificial piles. The results showed that the scour depth for single pier with debris is larger than that of pier without debris. They found that, in sacrificial piles with debris, the scour depth increased significantly compared to the sacrificial piles without debris.

In this study, the flow and scour pattern near bridge piers with different configurations (single, tandem, side by side and piers group 2 × 2) were investigated in two cases of with and without debris. In the debris tests, the effect of debris shapes (cylindrical, rectangular, triangular), thickness, effective lengths and positions were studied. The results were compared with the results of other researchers and finally, some modification were done on the common empirical formula used for predicting of scour depth.

2. Materials and Methods

2.1 Experimental Equipment

This research was carried out at the Hydraulic Laboratory of Shahid Bahonar University of Kerman (HLUK), Iran. A rectangular recirculating flume with steel bottom and glass walls with 8 m length, 0.8 m width and 0.6 m depth was used for conducting the experiments. The schematic representation of the experimental set-up is shown in Fig. 1. In the laboratory, the water was supplied from an under-floor sump using two centrifugal pumps and thereafter was fed to the flume through 101.6 mm diameter pipe with an adjustable valve for controlling the discharge. The discharge was measured with a volumetric flow meter with stated accuracy of 1%. Provisions were made at the inlet to the flume to ensure uniform flow and to diminish the surface waves,

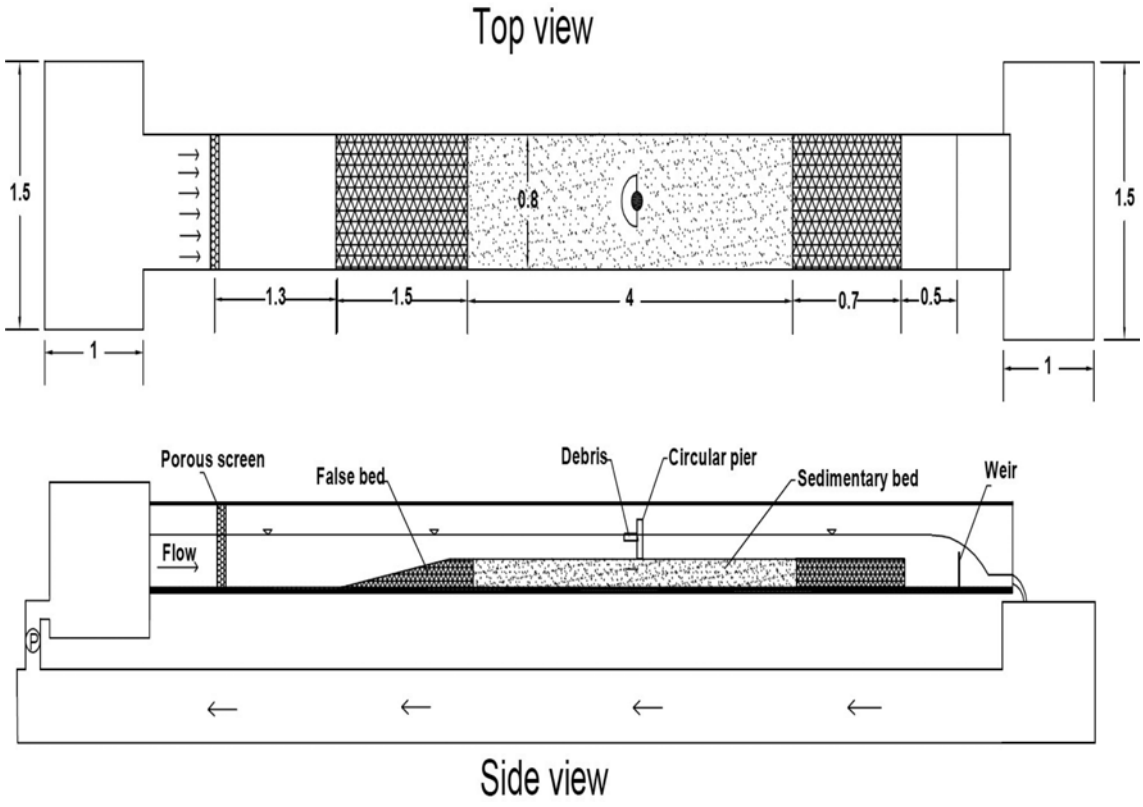

Fig. 1. Schematic Representation of the Experimental Set-up

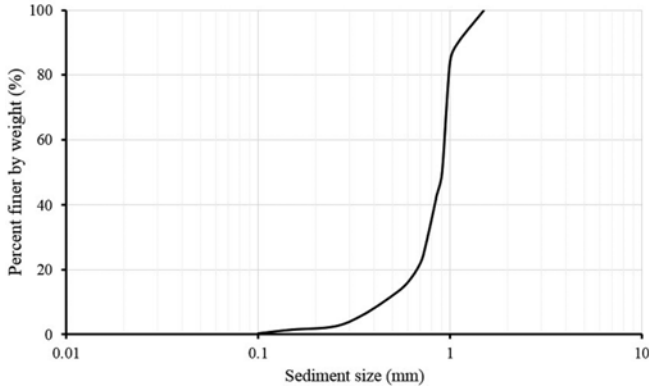

Fig. 2. Size Distribution Curve of the Bed Materials

vortices and turbulence caused by pump fluctuations. After that, the outflow from flume was returned to the sump and recirculated through this system. False bottom with 4 m length, 0.16 m depth and 0.8 m width was used to insert the bridge pier and the bed material, as shown in Fig. 1. The bed material was non-cohesive sediments with median diameter (D_{50}) of 0.91 mm, and geometric standard deviation (σ_g) of 1.27. The sediment size distribution curve of the bed materials has been demonstrated in Fig. 2. It should be noted that, Raudkivi and Ettema (1983) recommended that the median diameter of the sediment particles should be larger than 0.7 mm to preventing the ripples formation. In addition, to eliminate the effect of non-uniformity of sediment on scour, the standard deviation of particles size should be less than 1.3 (Chiew and Melville, 1987).

A metal cylindrical pier with diameter of 0.03 m was used in the tests. All tests of this study were conducted at clear water sediment transport condition, i.e., the ratio of mean flow velocity to critical velocity was less than 1. In addition, to avoid the roughness effects on the scour depth, the flow depth should be greater than 20 mm (Oliveto and Hager, 2002). Furthermore, the ratio of pier diameter to flow depth should be less than 0.7 to prevent it from affecting the scour depth (Melville and Hadfield, 1999). Considering the above recommendations, the flow rate

Table 1. Experimental Tests

Test	Debris shape	Configuration	D_d	T_d	h_d	G	Af	Ap
1	N	S	-	-	-	-	-	-
2	N	T	-	-	-	0.1	-	-
3	N	SS	-	-	-	0.1	-	-
4	N	G (2×2)	-	-	-	0.1	-	-
5	Tri	S	0.2	0.03	0.02	-	0.006	0.01
6	Tri	T	0.2	0.03	0.02	0.1	0.006	0.01
7	Tri	SS	0.2	0.03	0.02	0.1	0.006	0.01
8	Tri	G (2×2)	0.2	0.03	0.02	0.1	0.006	0.01
9	Cyl	S	0.2	0.03	0.02	-	0.006	0.0157
10	Cyl	T	0.2	0.03	0.02	0.1	0.006	0.0157
11	Cyl	SS	0.2	0.03	0.02	0.1	0.006	0.0157
12	Cyl	G (2×2)	0.2	0.03	0.02	0.1	0.006	0.0157
13	Rec	S	0.2	0.03	0.02	-	0.006	0.02
14	Rec	T	0.2	0.03	0.02	0.1	0.006	0.02
15	Rec	SS	0.2	0.03	0.02	0.1	0.006	0.02
16	Rec	G (2×2)	0.2	0.03	0.02	0.1	0.006	0.02
17-19	Tri, Cyl, Rec	S	0.1	0.03	0.02	-	0.003	0.001
20-22	Tri, Cyl, Rec	T	0.1	0.03	0.02	0.1	0.003	0.001
23-25	Tri, Cyl, Rec	SS	0.1	0.03	0.02	0.1	0.003	0.001
26-28	Tri, Cyl, Rec	G (2×2)	0.1	0.03	0.02	0.1	0.003	0.001
29-31	Tri, Cyl, Rec	S	0.1	0.03	0.02	-	0.003	0.003, 0.004, 0.005
32-34	Tri, Cyl, Rec	T	0.1	0.03	0.02	0.1	0.003	0.003, 0.004, 0.005
35-37	Tri, Cyl, Rec	SS	0.1	0.03	0.02	0.1	0.003	0.003, 0.004, 0.005
38-40	Tri, Cyl, Rec	G (2×2)	0.1	0.03	0.02	0.1	0.003	0.003, 0.004, 0.005
41-43	Tri, Cyl, Rec	S	0.2	0.03	0.02	-	0.006	0.006, 0.009, 0.011
44-46	Tri, Cyl, Rec	T	0.2	0.03	0.02	0.1	0.006	0.006, 0.009, 0.011
47-49	Tri, Cyl, Rec	SS	0.2	0.03	0.02	0.1	0.006	0.006, 0.009, 0.011
50-52	Tri, Cyl, Rec	G (2×2)	0.2	0.03	0.02	0.1	0.006	0.006, 0.009, 0.011
53-55	Tri, Cyl, Rec	S	0.3	0.03	0.02	-	0.009	0.016, 0.025, 0.031
56-58	Tri, Cyl, Rec	T	0.3	0.03	0.02	0.1	0.009	0.016, 0.025, 0.031
59-61	Tri, Cyl, Rec	SS	0.3	0.03	0.02	0.1	0.009	0.016, 0.025, 0.031
62-64	Tri, Cyl, Rec	G (2×2)	0.3	0.03	0.02	0.1	0.009	0.016, 0.025, 0.031

Table 1. (continued)

Test	Debris shape	Configuration	D_d	T_d	h_d	G	Af	Ap
65-67	Tri, Cyl, Rec	S	0.3	0.03	0.02	-	0.009	0.023, 0.035, 0.045
68-70	Tri, Cyl, Rec	T	0.3	0.03	0.02	0.1	0.009	0.023, 0.035, 0.045
71-73	Tri, Cyl, Rec	SS	0.3	0.03	0.02	0.1	0.009	0.023, 0.035, 0.045
74-76	Tri, Cyl, Rec	G (2×2)	0.3	0.03	0.02	0.1	0.009	0.023, 0.035, 0.045
77-79	Tri, Cyl, Rec	S	0.2	0.015	0.01	-	0.003	0.01, 0.016, 0.02
80-82	Tri, Cyl, Rec	T	0.2	0.015	0.01	0.1	0.003	0.01, 0.016, 0.02
83-85	Tri, Cyl, Rec	SS	0.2	0.015	0.01	0.1	0.003	0.01, 0.016, 0.02
86-88	Tri, Cyl, Rec	G (2×2)	0.2	0.015	0.01	0.1	0.003	0.01, 0.016, 0.02
89-91	Tri, Cyl, Rec	S	0.2	0.03	0.02	-	0.006	0.01, 0.016, 0.02
92-94	Tri, Cyl, Rec	T	0.2	0.03	0.02	0.1	0.006	0.01, 0.016, 0.02
95-97	Tri, Cyl, Rec	SS	0.2	0.03	0.02	0.1	0.006	0.01, 0.016, 0.02
98-100	Tri, Cyl, Rec	G (2×2)	0.2	0.03	0.02	0.1	0.006	0.01, 0.016, 0.02
101-103	Tri, Cyl, Rec	S	0.2	0.06	0.03	-	0.012	0.01, 0.016, 0.02
104-106	Tri, Cyl, Rec	T	0.2	0.06	0.03	0.1	0.012	0.01, 0.016, 0.02
107-109	Tri, Cyl, Rec	SS	0.2	0.06	0.03	0.1	0.012	0.01, 0.016, 0.02
110-112	Tri, Cyl, Rec	G (2×2)	0.2	0.06	0.03	0.1	0.012	0.01, 0.016, 0.02
113-115	Tri, Cyl, Rec	S	0.2	0.07	0.04	-	0.014	0.01, 0.016, 0.02
116-118	Tri, Cyl, Rec	T	0.2	0.07	0.04	0.1	0.014	0.01, 0.016, 0.02
119-121	Tri, Cyl, Rec	SS	0.2	0.07	0.04	0.1	0.014	0.01, 0.016, 0.02
122-124	Tri, Cyl, Rec	G (2×2)	0.2	0.07	0.04	0.1	0.014	0.01, 0.016, 0.02
125-127	Tri, Cyl, Rec	S	0.2	0.08	0.04	-	0.016	0.01, 0.016, 0.02
128-130	Tri, Cyl, Rec	T	0.2	0.08	0.04	0.1	0.016	0.01, 0.016, 0.02
131-133	Tri, Cyl, Rec	SS	0.2	0.08	0.04	0.1	0.016	0.01, 0.016, 0.02
134-136	Tri, Cyl, Rec	G (2×2)	0.2	0.08	0.04	0.1	0.016	0.01, 0.016, 0.02
137-140	Cyl	S or T or SS or G (2×2)	0.2	0.03	0	0.1	0.006	0.0157
141-144	Cyl	S or T or SS or G (2×2)	0.2	0.03	0.02	0.1	0.006	0.0157
145-148	Cyl	S or T or SS or G (2×2)	0.2	0.03	0.03	0.1	0.006	0.0157
149-152	Cyl	S or T or SS or G (2×2)	0.2	0.03	0.04	0.1	0.006	0.0157
153-156	Cyl	S or T or SS or G (2×2)	0.2	0.03	0.05	0.1	0.006	0.0157
157-160	Cyl	S or T or SS or G (2×2)	0.2	0.03	0.06	0.1	0.006	0.0157
161-164	Cyl	S or T or SS or G (2×2)	0.2	0.03	0.07	0.1	0.006	0.0157
165-168	Cyl	S or T or SS or G (2×2)	0.2	0.03	0.08	0.1	0.006	0.0157
169-172	Cyl	S or T or SS or G (2×2)	0.2	0.03	0.09	0.1	0.006	0.0157
173-176	Cyl	S or T or SS or G (2×2)	0.2	0.03	0.1	0.1	0.006	0.0157
177-180	Cyl	S or T or SS or G (2×2)	0.2	0.03	0.11	0.1	0.006	0.0157
181-184	Cyl	S or T or SS or G (2×2)	0.2	0.03	0.11	0.01	0.006	0.0157
185-188	Cyl	S or T or SS or G (2×2)	0.2	0.03	0.11	0.02	0.006	0.0157
190-192	Cyl	S or T or SS or G (2×2)	0.2	0.03	0.11	0.03	0.006	0.0157
193-196	Cyl	S or T or SS or G (2×2)	0.2	0.03	0.11	0.06	0.006	0.0157
197-200	Cyl	S or T or SS or G (2×2)	0.2	0.03	0.11	0.08	0.006	0.0157
201-204	Cyl	S or T or SS or G (2×2)	0.2	0.03	0.11	0.09	0.006	0.0157
205-208	Cyl	S or T or SS or G (2×2)	0.2	0.03	0.11	0.12	0.006	0.0157
209-212	Cyl	S or T or SS or G (2×2)	0.2	0.03	0.11	0.18	0.006	0.0157
213-216	Cyl	S or T or SS or G (2×2)	0.2	0.03	0.11	0.24	0.006	0.0157
217-220	Cyl	S or T or SS or G (2×2)	0.2	0.03	0.11	0.3	0.006	0.0157

N = No debris, Tri = Triangular debris, Cyl = Cylindrical debris, S = Single, T = Tandem, SS = Side by Side, G (2 × 2) = Group pier (2 × 2), Ap = plan area of debris, Af = front area of debris (upstream face area).

was adjusted at 32 *l/s*. The depth of flow was kept constant using a weir at the end of the flume. The bed topography and the final scour profiles around the pier were measured longitudinally and transversally using Leica DISTO D2 laser distance measurer with ±0.1 mm of reading accuracy. In addition, photographs were taken with *Canon Powershot SX 160 IS* camera during the experiments and used to visualize the scour processes.

This study considered different combinations of debris configuration and piers number, as well as, a range of debris geometrical characteristics including debris shape, thickness,

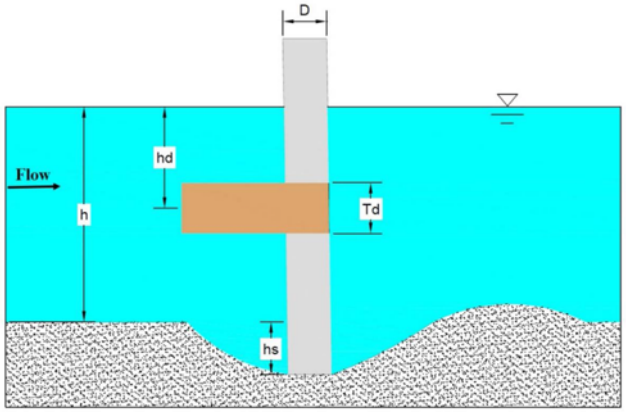

Fig. 3. Schematic Representation of Pier Scour in the Presence of Debris

effective length, and submergence ratio. The tests of this study have been provided in Table 1. The parameters mentioned in this table has been demonstrated in Fig. 3.

2.2 Tests Procedure

The main purpose of this research was to study the mechanism of piers group scour in the presence of debris. In total, 220 experiments were performed to investigate the effect of debris geometrical properties on the dimensions of scour hole. The tests have been carried out with debris accumulation upstream of piers group, though single pier were investigated in literature, i.e., Melville and Dongol (1992) (cylindrical debris) or Zevenbergen *et al.*, 2006 (triangular debris). Before each experiment the bed was carefully leveled around the bridge pier and the debris was fixed at a given distance from the bed. After that, the flume was slowly filled up with water until the water surface reached to a depth of 12 cm over the bed. All tests were performed under constant discharge and head. The duration of the experiments was determined by an equilibrium test. This test was run for 24h, and during the test, the temporal variations of scour hole were recorded by a camera. Analysis of the recorded video revealed that, after 8 hours from the beginning of the experiment, the variations of scour depth was less than 1 mm over a period of 3h. Therefore, the time 8h was taken as the equilibrium condition (Kumar *et al.*, 1999). Then the pump was turned off and the water in the flume was drained completely and then the geometrical dimensions of scour hole were measured.

3. Results and Discussions

In this section, the experimental observations are reported for single pier (*S*), tandem piers (*T*), side by side piers (*SS*) and piers group (*G* 2 × 2), respectively. The flow pattern and scour processes are reported for each of the configurations. After that, the effect of debris geometrical characteristics on the flow behavior and scour phenomenon is reported and interpreted for each pier configurations.

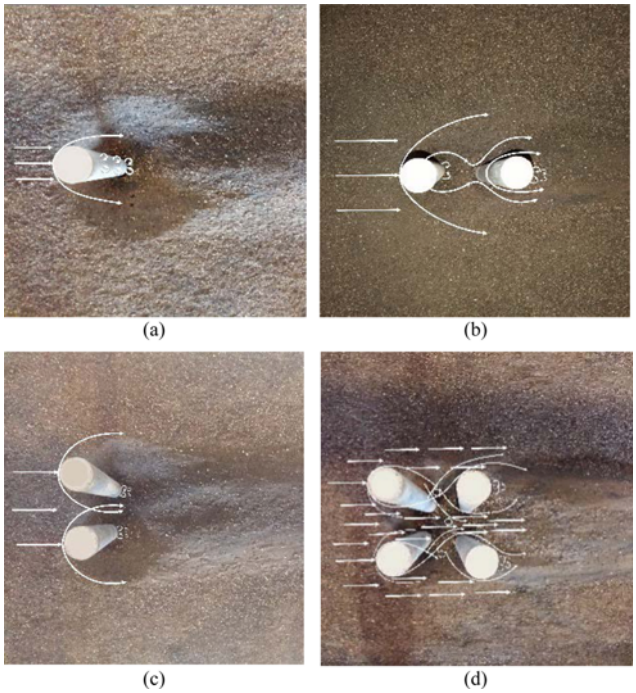

Fig. 4. Schematic Representation of Flow Pattern: (a) Single Pier, (b) Tandem Pier, (c) Side by Side Pier, (d) Group Pier (2 × 2)

3.1 Mechanism of Scour at Piers Without Debris

As previously said, four different types of experiment were conducted in this study including single pier cases, tandem pier cases, side by side pier cases and piers group cases, in two conditions of with and without debris accumulation.

In single pier tests, when the flow collided with the upstream face of pier, a vertical stagnation pressure gradient formed along the face, led to generating a down flow jet which pushed the bed and eroded the sediments. Thereafter, the primary vortex which was formed around the pier eroded a great part of bed materials and developed the scour hole. Simultaneously, the wake vortices created by the separation of flow from pier corners, sucked up the materials from scour hole and carried it out toward the downstream (Fig. 4(a)). In tandem configuration (Fig. 4(b)), the scour processes was somewhat different from that of single pier. In this case, the front pier was subjected to a substantial scour due to the reinforcement effect of the rear pier. The lowering of the bed level at the rear pier facilitated the escape of sediments from the front pier scour hole and leads to a deeper scour at front pier. In other hand, the front pier protected the rear pier from scour by deflecting the high velocity flow and creating a wake region behind it.

In side by side configuration (Fig. 4(c)), a large interference occurred between the piers which caused generation of a strong gap flow between the two piers, led to formation of compressed horseshoe vortices between the piers. Observations are well consistent with those of Ataei-Ashtiani and Beheshti (2006) and Madadi *et al.* (2016). In piers group (2 × 2) configuration (Fig. 4(d)), complex interactions occurred among the flow, sediment

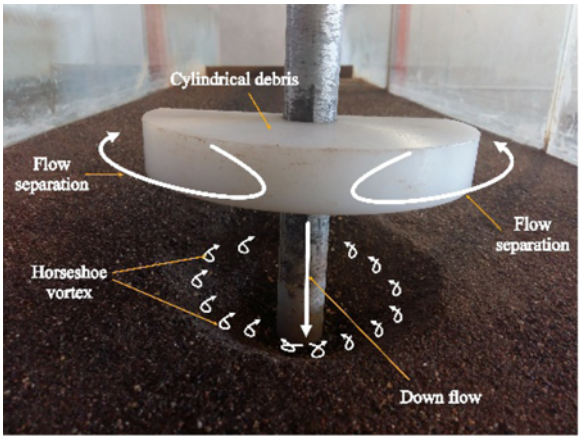

Fig. 5. Schematic Representation of Flow Pattern Around the Pier with Debris

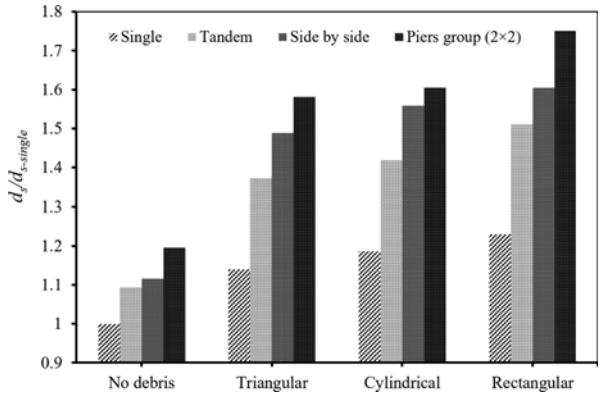

Fig. 6. Variations of Relative Scour Depth vs. Debris Shape

and piers. Strong gap flow in combination with compressed horseshoe vortices, caused scour of a large amount of sediments from the piers surroundings.

3.2 Mechanism of Scour at Piers with Debris

In the presence of debris accumulation upstream the pier, the scour processes changes significantly rather than of pier without debris. As shown in Fig. 5, debris alter the approaching flow pattern, force it to dive down along the front face of the pier. So a plunging jet is established that moves to the sedimentary bed and scours a large amount of sediments from the scour hole. In this case, stronger wake vortices form behind the pier which easies the conveyance of eroded sediments from the scour hole toward downstream. In addition, horseshoe vortices propagate in a larger area than the pier without debris, cause formation of a large scour hole.

The strength of the plunging jet depends on the geometrical and positional properties of debris. Followings, the effect of shape, thickness and position of debris on the dimensions of scour hole is investigated.

3.2.1 Effect of Debris Shape

As said, three debris shapes of triangular (Tri), rectangular (Rec) and cylindrical (Cyl) were tested in this study. Fig. 6 shows the effect of debris shape on the relative scour depth. As indicated, in all piers configurations, the maximum scour depth was observed in the rectangular debris, and the minimum one was belonged to the triangular debris. The values of $d_s/d_{s\text{-}single}$ for piers group (2 × 2) configuration were obtained 1.19, 1.58, 1.61, and 1.75 for no debris (N), Tri, Cyl and Rec, respectively (d_s and $d_{s\text{-}single}$ denote the maximum scour depth in each condition and the maximum scour depth single pier without debris respectively). In other word, the maximum relative depth at pier with rectangular debris was 47% more than that of no debris with the same configuration (piers group (2 × 2)). Similar results were obtained for other configurations.

The cause of larger scour depth at the pier(s) with rectangular debris was that, the flow streamlines after colliding with the rectangular debris deflected dramatically, led to more flow separation and establishment of stronger wake vortices behind the pier(s). But, in the triangular shape, because of its upstream sharp edge, the flow separation was less than two other shapes, so, weaker vortices formed behind the pier.

3.2.2 Effect of Debris Position

For all the experiments, debris was placed at different distances from the flow surface. Here, the results of cylindrical debris are reported. The results are consistent for other debris shapes.

The debris was mounted on the pier at eleven relative distances (h_d/h) of 0, 0.12, 0.21, 0.3, 0.38, 0.46, 0.54, 0.63, 0.71, .79 and 0.88 (h_d and h denote the debris center distances from the flow surface and the flow depth respectively). It was found that, the maximum scour depth increased by increasing the h_d/h, and reached to its maximum value at h_d/h = 0.46, then it decreased and eventually it reached to a smaller value than the pier(s) without the debris (Fig. 7). In other word, by increasing distance of debris from the flow surface from h_d/h = 0 to h_d/h = 0.46, the strength of down flow jet increased, while, with further increase of h_d/h, the debris caused decreasing of scour. For h_d/h = 0.88, the debris acted as a collar, thereby reduced the strength of down

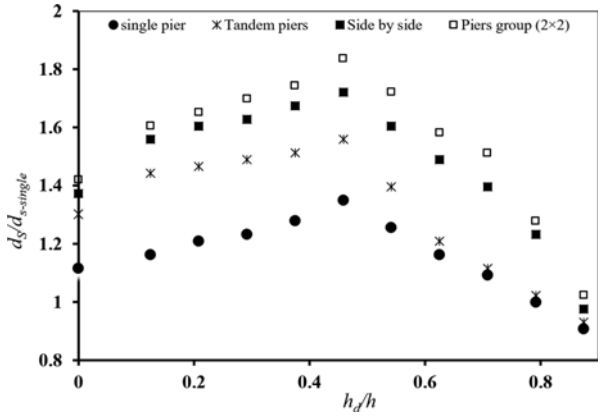

Fig. 7. Variations of Relative Scour Depth vs. Debris Relative Submerged Ratio

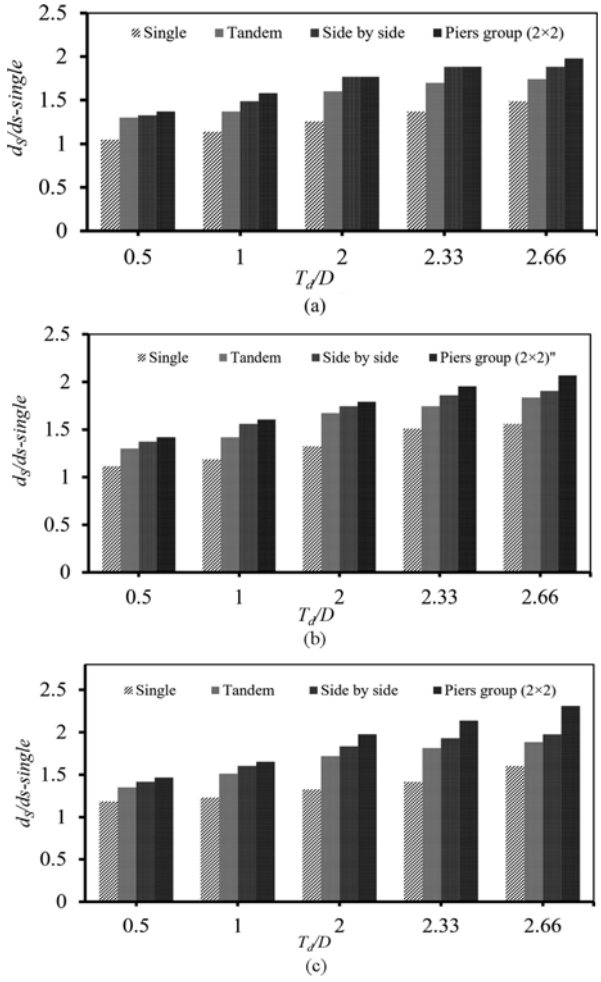

Fig. 8. Variations of Relative Scour Depth Debris vs. Relative Thickness: (a) Triangular, (b) Cylindrical, (c) Rectangular

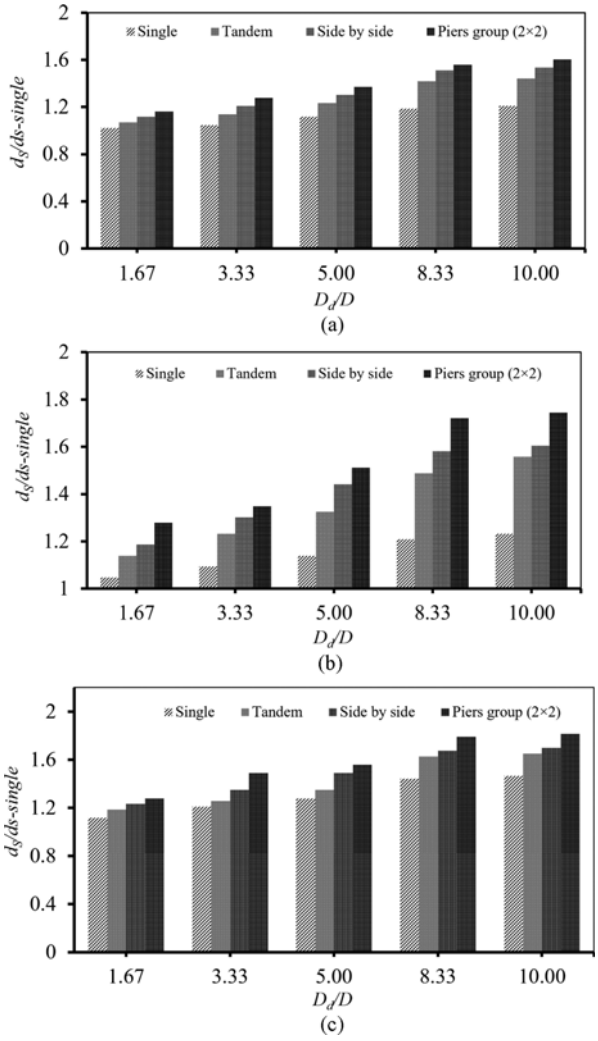

Fig. 9. Variations of Relative Scour Depth Debris vs. Relative Effective Length: (a) Triangular, (b) Cylindrical, (c) Rectangular

flow (sheltering effect) and mitigated the scouring processes. As shown in Fig. 7, the overall shape of variations of scour depth versus h_d/h were similar in all configurations but the corresponding values was largest for piers group (2 × 2), after that, side by side piers, tandem piers, and single piers, respectively.

3.2.3 Effect of Debris Thickness

Figure 8 demonstrates the effect of debris thickness on the maximum scour depth. It is observed that more the debris thickness, more the depth of scour hole. For the cylindrical debris, as the relative thickness of debris increased from 0.5 to 2.66, the scour depth increased 56%, 84%, 91% and 107% at single, tandem, side by side, piers group (2 × 2) respectively. For the rectangular debris, the scour depth increased 60%, 88%, 98% and 144% for the same order of debris shape. For the triangular debris, it was observed that by increasing the relative thickness of debris from 0.5 to 2.66, the scour depth increased 49%, 74%, 88% and 98% at single, tandem, side by side, piers group (2 × 2), respectively.

As the thickness of debris increases, a wider area of debris is exposed to the approaching flow, therefore, a larger down flow is directed to bed and stronger horseshoe vortices establishes around the pier, resulting more scour depth.

3.2.4 Effect of Debris Effective Length

This series of experiments were performed to investigate the effect of length (D_d) of the debris on the maximum depth of scour hole. Five different effective lengths of 0.05, 0.1, 0.15, 0.25 and 0.3 m were used in the experiments. As shown in Fig. 9, the depth of scour hole primarily increases by increasing the debris effective length, but it become constant for the high values of effective length. It means that, as the effective length of debris reaches to a certain value, the variations of D_d has negligible effect on the depth of scour hole. From Fig. 9 it can be seen that, by increasing the effective length of rectangular debris from 1.66 to 10 the $ds/d_{s\text{-}single}$ increases 47%, 65%, 70%, and 81% in single, tandem, side by side and piers group (2 × 2) configuration. This trend was observed in all other debris shapes (Fig. 9(a)-(c)).

3.3 Effect of Piers Spacing on the Scour Processes

For all piers group configurations, the effect of piers spacing

(G) on the scour depth was investigated in two cases of with and without debris (Fig. 10). The results showed that, for the tandem piers, the maximum scour depth increases with increasing G/D, and reaches the maximum value at $G/D = 2.5$, Then it decreases, and eventually it reaches its single-pier value. The maximum scour depth at tandem configuration was 16% higher than the single pier value at $G/D = 2.5$. The horseshoe vortices around the rear pier facilitated the scouring of materials from surroundings of front pier and caused formation of a deeper scour hole.

In the case of side by side piers, with increasing the G/D, the scour depth decreased. Based on the observations, the scour depth for side by side configuration with $G/D = 0.25$, was about 41% more than that of single pier.

For piers group (2 × 2) configuration, by increasing G/D, the scour depth decreased. The maximum scour depth was observed at $G/D = 0.25$, ($ds/d_{s\text{-}single} = 1.56$), about 56% more than that of single pier.

It was found that for all values of G/D, the maximum scour depth occurred at piers group (2 × 2), side by side piers, tandem piers and single pier, with descending order. This is due to the increased size of the horseshoe vortices, the strong gap flow between the two adjacent piers, and the complex interactions of flow, sediment and piers with increasing the piers number.

In the presence of debris upstream of the piers (all the configurations), the overall trend of scour processes was almost similar to that of piers without debris, but, the depth of scour hole increased significantly. Fig. 10(a), 10(b) demonstrates the variations of relative depth of scour hole versus the relative spacing of piers. In the presence of debris, the strength of compressed vortices were further increased in compare with the piers without debris.

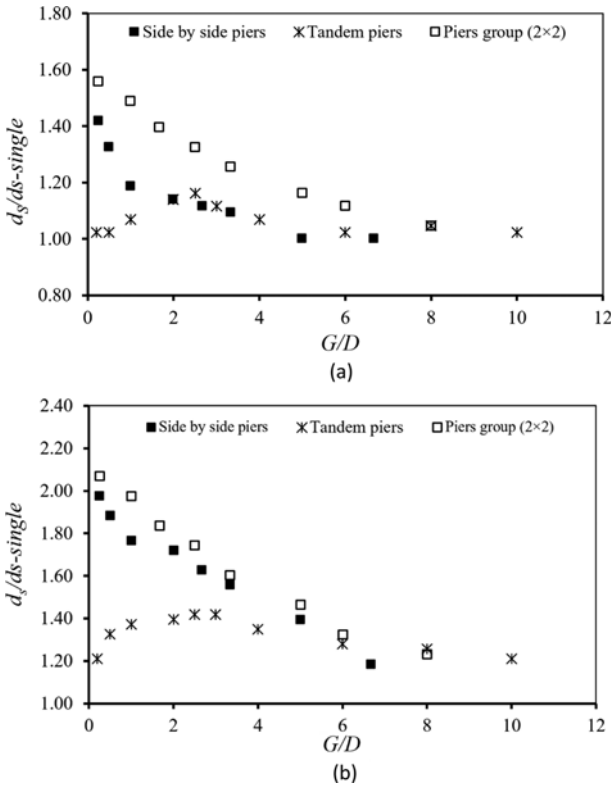

Fig. 10. Variations of Relative Scour Depth vs. Relative Spacing in pier: (a) Without Debris, (b) with Debris

3.4 Predicting of the Maximum Scour Depth

Several empirical formula have been presented for predicting the maximum scour depth at single piers with debris. Based on their experimental data, Melville and Dongol (1992) proposed Eq. (1) to estimate the maximum scour depth at pier with debris accumulation:

$$d_s = k.D_e \tag{1}$$

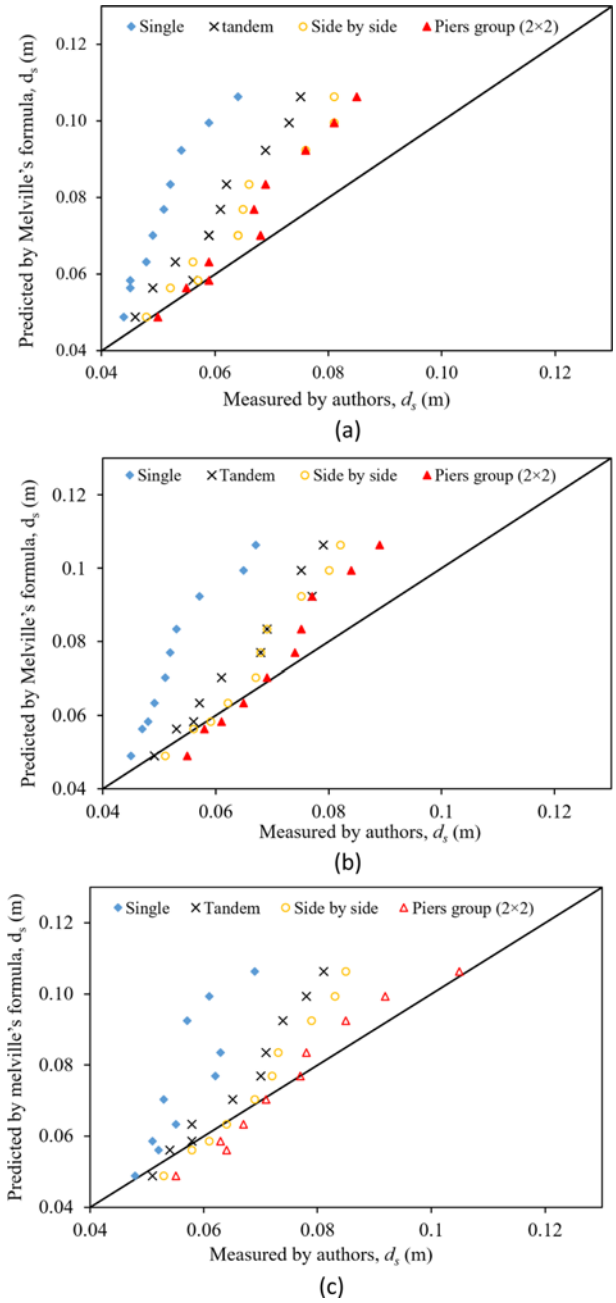

Fig. 11. Predicted Scour Depth by Melville's Formula vs. Measured by Authors: (a) Triangular, (b) Cylindrical, (c) Rectangular

Table 2. Empirical Equations for Predicting of the Maximum Scour Depth

Configuration	Shape		k
single	All	y/De<2.3	1.56
		y/De>2.3	1.92
Tandem	Cyl, Tri.		2.04
	Rec.	y/De<2.3	1.92
		y/De>2.3	2.4
Side by side	All	y/De<2.3	2.04
		y/De>2.3	2.4
Group pier (2×2)	All	y/De<2.3	2.2
		y/De>2.3	2.4

In which,

$$D_e = \frac{0.52T_dD_d + (y - 0.52T_d)D}{y} \quad (2)$$

Where, k is a factor that represents the effective parameters of scour, D_e is the effective length of pier with debris accumulation, D = pier diameter, D_d = width of debris, T_d = thickness of debris and y = flow depth.

Melville and Dongol (1992) determined the value of k equal to 2.4 for y/D_e >2.6. While, recent researches revealed that Eq. (1) over predict the maximum scour depth in compare with the observed data (Pagliara and Carnacina, 2011; Lagasse *et al.*, 2011). Park *et al.* (2016b) modified equation (1) by changing the value of k, for the experimental conditions of their study and concluded that the results of Melville's modified formula was well fitted with the results of their laboratory data.

In this study, the results of experimental tests were compared with the results of Eq. (1), as shown in Fig. 11, It was found that, in the case of single pier, Melville's formula over predicted the maximum scour depth as already reported by Pagliara and Carnacina (2010) and Lagasse *et al.* (2011). For tandem piers and side by side piers, the observed data were somewhat close to the result of Eq. (1). For piers group (2 × 2), the Melville's formula (Eq. (1)) was well capable to predict the maximum scour depth. The results showed that, for the single pier with debris, as $y/D_e < 2.3$ the measured k value was consistent with the $k = 1.56$ proposed by Park *et al.* (2016b), but for $y/D_e \geq 2.3$, the value of $k = 1.92$ showed more accurate prediction. Furthermore, k value proposed by Melville and Dongol (1992), showed satisfactory predictions for $y/D_e \geq 2.3$ in all cases of (I) tandem piers with rectangular debris, (II) side by side piers with all debris shapes, and (III) piers group (2 × 2) with all debris shapes. The detailed values of k were presented in Table 2.

4. Conclusions

In this experimental study, the flow behavior and scour pattern around different configurations of bridge piers including single pier, side by side piers, tandem piers and piers group (2 × 2), were investigated. The experiments were carried out for two cases of with- and without debris accumulation upstream of the pier(s). In summary, the following findings were obtained based on the analysis of the experimental observations:

1. In piers with tandem configuration, a deeper scour hole created at front pier. In this case, the front pier protected the rear pier from scour. In side by side configuration, a strong gap-flow generated between the piers, led to formation of compressed horseshoe vortices between the piers. In all experiments, the maximum scour depth was observed at piers group (2 × 2) configuration.
2. For all pier configurations, the accumulation of debris upstream of the pier(s), increased the depth of scour hole. In the presence of debris, the strength of compressed vortices were further increased compared with the piers without debris. For example, the relative maximum depth of scour hole at piers group (2 × 2), with $G/D = 3.33$, and rectangular debris ($h_d/h = 0.125$, $D_d/D = 6.67$ and $T_d/D = 1$) was 47% more than pier without debris, for the same configuration.
3. By increasing the distance of debris from the flow surface, the maximum depth of scour hole increased primarily, thereafter decreased and eventually reached to a smaller value than the pier(s) without the debris.
4. The results indicated that more the debris thickness, more the depth of scour hole. For the cylindrical debris with $h_d/h = 0.125$ and $D_d/D = 6.67$, as the relative thickness of debris increased from 0.5 to 2.66, the scour depth increased 56%, 84%, 91% and 107% at single, tandem, side by side, and piers group (2 × 2), respectively, all for $G/D = 3.33$.
5. By increasing the debris effective length, the depth of scour hole increased firstly, and then became constant for high values of effective length. For example, as the effective length of rectangular debris with $h_d/h = 0.125$ and $T_d/D = 1$, increased from 1.66 to 10, the $ds/d_{s\text{-}single}$ increased up to 47%, 65%, 70%, and 81% in single, tandem, side by side and piers group (2 × 2) configuration, respectively, all for $G/D = 3.33$.
6. The variations of maximum scour depth versus piers relative spacing (G/D) was depended on pier configuration. For tandem piers, the maximum scour depth increased with increasing G/D, and reached the maximum value at $G/D = 2.5$ (16% more than the single pier), Then it decreased, and eventually reached its single-pier value. In side by side piers and piers group (2 × 2), with increasing the G/D, the scour depth decreased. In the presence of debris at upstream of the piers (for all the configurations), the overall trend of scour processes was almost similar to that of piers without debris, but, the value of scour depth increased, significantly.
7. Comparison of experimental data with common empirical equations indicated that though Melville's formula over predicted the maximum scour depth at single pier, it was well capable to predict the maximum scour depth at piers group (2 × 2). Also, Melville's formula could satisfactorily predict the scour depth at tandem and side by side piers. Based on the measured data at the present study, some modifications were applied to the previous empirical formula.

Notations

The following symbols are used in this paper:

D = Pier diameter.
D_e = Effective length of the pier with debris.
D_d = Width of floating debris.
T_d = Submerged debris thickness.
$d_{s\text{-}single}$ = The maximum depth of scour at single pier.
d_s = The maximum depth of scour.
D_{50} = Median size of bed material.
G = Spacing between the pier.
Q = Discharge.
h = Flow depth.
h_d = Debris center distances from the flow surface.
N = No debris.
S = Single.
T = Tandem.
SS = Side by side.
$G\,(2 \times 2)$ = piers group (2×2)
k = Scour coefficient.
Rec = Rectangular debris.
Tri = Triangular debris.
Cyl = Cylindrical debris.

References

Abbe, T. B. and Montgomery, D. R. (1996). "Large woody debris jams, channel hydraulics and habitat formation in large rivers." *Regulated Rivers: Research & Management*, Vol. 12, pp. 201-201.

Ataie-Ashtiani, B. and Beheshti, A. A. (2006). "Experimental investigation of clear-water local scour at pile groups." *Journal of Hydraulic Engineering*, Vol. 132, No. 10, pp. 1100-1104.

Bradley, J. B., Richards, D. L., and Bahner, C. D. (2005). *Debris control structures-Evaluation and countermeasures*, FHWA-IF-04-016, HEC-9, Federal Highway Administration, Washington, DC.

Braudrick, C. A., Grant, G. E., Ishikawa, Y., and Ikeda, H. (1997). "Dynamics of wood transport in streams: A flume experiment." *Earth Surf. Processes Landforms*, Vol. 22, No. 7, pp. 669-683.

Briaud, J. L., Chen, H. C., Chang, K. A., Chen, X., and Oh, S. J. (2006). "Scour at bridges due to debris accumulation: A review." *Proc., ICSE 2006, 3rd Int. Conf. on Scour and Erosion*, Amsterdam, the Netherlands.

Chang, F. F. M. and Shen, H. W. (1979). *Debris Problems in the River Environment,* FHWA-RD-79-62.

Chiew, Y. M. and Melville, B. W. (1987). "Local scour around bridge piers." *Journal of Hydraulic Research*, Vol. 25, No. 1, pp. 15-26.

Diehl, T. H. (1997). *Potential drift accumulations at bridges*, Report RD-97-28, Federal Highway Administration, U.S. Dept. of Transportation, McLean, VA.

Franzetti, S., Radice, A., Rabitti, M., and Rossi, G. (2011). "Hydraulic design and preliminary performance evaluation of countermeasure against debris accumulation and resulting local pier scour on river po in Italy." *J. Hydraul. Eng.,* 10.1061/(ASCE)HY.1943-7900.0000340, 615-620.

Kattell, J. and Eriksson, M. (1998). *Bridge scour evaluation: Screening, analysis, and countermeasures*, Gen. Tech, Rep. 9877-1207-SDTDC. U.S. Department of Agriculture, San Dimas, CA.

Kumar, V., Raju, K. G. R., and Vittal, N. (1999). "Reduction of local scour around bridge piers using slots and collars." *Journal of Hydraulic Engineering*, Vol. 125, No. 12, pp. 1302-1305.

Lagasse, P. F., Clopper, P. E., and Zevenbergen, L. W. (2010). *Effects of Debris on Bridge Pier Scour*, NCHRP Report 653, Transportation Research Board, National Academies of Science, Washington, D.C.

Laursen, E. M. and Toch, A. (1956). *Scour around bridge piers and abutments*, Bulletin No. 4, Iowa Highways Research Board, Ames, Iowa.

Lyn, D. A., Cooper, T., Yi, Y. K., Sinha, R., and Rao, A. R. (2003). "Debris accumulation at bridge crossings: Laboratory and field studies." *Joint Transportation Research Program*, Report No. FHWA/IN/JTRP-2003/10.

Madadi, M. R., Rahimpour, M., and Qaderi, K. (2016). "Sediment flushing upstream of large orifices: An experimental study." *Flow Measurement and Instrumentation*, Vol. 52, pp.180-189.

Melville, B. W. and Coleman, S. E. (2000). "Bridge scour." *Water Resources Publications*, Highlands Ranch, CO.

Melville, B. W. and Dongol, D. M. (1992). "Bridge pier scour with debris accumulation." *J. Hydraul. Eng.*, Vol. 118, No. 9, pp. 1306-1310.

Melville, B. W. and Hadfield, A. C. (1999). "Use of sacrificial piles as pier scour countermeasures." *Journal of Hydraulic Engineering*, Vol. 125, No. 11, pp. 1221-1224.

Mueller, D. S. and Parola, A. C. (1998). "Detailed Scour Measurements around a Debris Accumulation." *ASCE. Water Resources Engineering*, pp. 234-239.

Oliveto, G. and Hager, W. H. (2002). "Temporal evolution of clear-water pier and abutment scour." *Journal of Hydraulic Engineering*, Vol. 128, No. 9, pp. 811-820.

Pagliara S. and Carnacina I. (2010). "Temporal scour evolution at bridge piers: Effect of wood debris roughness and porosity." *Journal of Hydraulic Research*, Vol. 48, No. 1, pp. 3-13.

Pagliara, S. and Carnacina, I. (2011). "Influence of large woody debris on sediment scour at bridge piers." *International Journal of Sediment Research*, Vol. 26, No. 2, pp. 121-136, DOI: 10.1016/S1001-6279(11)60081-4.

Park, J. H., Sok, C., Park, C. K., and Kim, Y. D. (2016a). "A study on the effects of debris accumulation at sacrificial piles on bridge pier Scour: I. Experimental Results." *KSCE Journal of Civil Engineering*, Vol. 20, No. 4, pp. 1546-1551, DOI: 10.1007/s12205-015-0207-5.

Park, J. H., Sok, C., Park, C. K., and Kim, Y. D. (2016b). "A study on the effects of debris accumulation at sacrificial piles on bridge pier Scour: II. Empirical formula." *KSCE Journal of Civil Engineering*, Vol. 20, No. 4, pp. 1552-1557, DOI: 10.1007/s12205-015-0208-4.

Parola, A. C., Apelt, C. J., and Jempson, M. A. (2000). *Debris forces on highway bridges*, Transportation Research Record, NCHRP Report No. 445, Transportation Research Board, Washington, D.C., ISBN: 0-309-06661-1.

Raudkivi, A. J. and Ettema, R. (1983). "Clear-water scour at cylindrical piers." *Journal of Hydraulic Engineering*, Vol. 109, No. 3, pp. 338-350.

Richardson, E. V. and Davis, S. R. (2001). *Evaluating Scour at Bridges, Fourth Edition*, Hydraulic Engineering Circular No. 18, Federal Highways Administration Publication No. FHWA NHI 01-001, Washington, D.C.

Wallerstein, N. P. (2003). "Dynamic model for constriction scour caused by large woody debris." *Earth Surf. Process. Landforms,* Vol. 28, pp. 49-68.

Zevenbergen, L. W., Lagasse, P. F., Clopper, P. E., and Spitz, W. J. (2006). *Effect of debris on bridge pier scour*, 3rd International conference on scour erosion, Amsterdam, The Nederland.